Toward the manipulation of a single spin in an AlGaAs/GaAs single-electron transistor

Sami Amasha*[a], Kenneth MacLean[a], Dominik Zumbühl[a], Iuliana Radu[a], Marc A. Kastner[a], Micah P. Hanson[b], Arthur C. Gossard[b]
[a] Department of Physics, Massachusetts Institute of Technology, Cambridge, MA 02139
[b] Materials Department, University of California, Santa Barbara 93106-5050

ABSTRACT

Single-electron transistors (SETs) are attractive candidates for spin qubits. An AlGaAs/GaAs SET consists of a confined two-dimensional droplet of electrons, called an artificial atom or quantum dot, coupled by tunnel barriers to two conducting leads. Controlling the voltages on the lithographic gates that define the quantum dot allows us to confine a single electron in the dot, as well as to adjust the tunnel barriers to the leads. By applying a magnetic field, we can split the spin-up and spin-down states of the electron by an energy $|g|\mu_B B$; the goal is to utilize coherent superpositions of these spin states to construct a qubit. We will discuss our attempts to observe electron spin resonance (ESR) in this system by applying magnetic fields at microwave frequencies. Observation of ESR would demonstrate that we can manipulate a single spin and allow us to measure the decoherence time T_2*.

Keywords: solid-state quantum computing, decoherence

1. INTRODUCTION

Lithographically defined AlGaAs/GaAs single-electron transistors (SETs) are attractive candidates for spin qubits[1]. An SET consists of a confined droplet of electrons called an artificial atom or quantum dot[2-4] coupled to conducting leads. SETs have proven to be a valuable tool for probing spin physics[5-8] in condensed matter systems. In particular the discovery[9,10] and subsequent study of the Kondo effect in SETs, including the singlet-triplet Kondo effect[11-13] and the ac Kondo effect[14], have demonstrated that SETs provide the ability to exert control over spin.

More recent experiments have demonstrated an even greater ability to control spin in quantum dots. By applying a magnetic field parallel to the dot, one can split the spin-up and spin-down states of the artificial atom by the Zeeman energy $|g|\mu_B B$. When the electron is prepared in the higher-energy spin state, the time necessary for the electron to relax back to the ground state is called T_1. Measurements by Elzerman, *et al.*[15] have shown that T_1 is on the order of 1 ms at 8 T and have also demonstrated the ability to do a single-shot read-out of the spin of an electron in a quantum dot. The relaxation time is expected to increase with decreasing magnetic field[16], and our own measurements have found T_1 times as long as 170 ms at a field of 1.75 T[17].

Although the excited spin state has a very long lifetime, the coherence time is shorter. Experiments on double quantum dots with one electron in each dot have probed the time necessary for a coherent superposition of spin states to become decoherent[18]. Until recently, it was not known whether the dominant decoherence process would be from the random magnetic field created by the magnetic moments of the Ga and As nuclei[19] or whether it would be from spin-orbit processes[16]. Measurements by Johnson *et al.*[18] have shown that the random nuclear fields are important: an electron on the dot sees a fluctuating field of approximately 3 mT, giving an inhomogenous decoherence time $T_2^* = |g| \mu_B B_{nuc}$ of 9 ns. However, further measurements by Petta, *et al.*[20] using a spin-echo technique have revealed that this random nuclear field can change fairly slowly: the decoherence time T_2 over which the random field changes are greater than 1 μs. This sets the timescale for which spins in a quantum dot become decoherent, and thus sets the timescales for manipulating the spin on the dot.

One proposed method for manipulation of the spin of an electron in a quatum dot is electron spin resonance (ESR)[21]. By applying a magnetic field parallel to the plane of the two-dimensional electron gas (2DEG), from which the

Quantum Information and Computation IV, edited by Eric J. Donkor, Andrew R. Pirich, Howard E. Brandt,
Proc. of SPIE Vol. 6244, 624419, (2006) · 0277-786X/06/$15 · doi: 10.1117/12.665548

dot is formed, one splits the spin-up and spin-down states of the artificial atom by the Zeeman energy $|g|\mu_B B$. Applying an oscillating magnetic field perpendicular to this static field causes an electron to flip its spin. This process is strongest at resonance, when the frequency of the oscillation (typically in the microwave region) is equal to the Zeeman energy for spin-splitting $|g|\mu_B B$, and decreases as the frequency (or alternatively the static magnetic field) is moved away from resonance. The width in frequency of the resonance is a measure of the inhomogenous decoherence rate $(T_2^*)^{-1}$. The goal is to use ESR to create and manipulate coherent superpositions of spin-up and spin-down states.

2. DEVICES

To fabricate our SETs we use an AlGaAs/GaAs heterostructure shown in figure 1a. This heterostructure has a 2DEG at the interface between the AlGaAs and GaAs with density of 2.2 x 10^{11} cm^{-2} and a mobility of 6.4 x 10^5 cm^2/Vs. Most importantly for our work, the heterostructure is very quiet, being mostly switch free.

Using electron beam lithography, we pattern nano-scale metallic gates on the surface of the heterostructure, shown in figure 1b. By applying a negative voltage to all the labeled gates in figure 1b except QG2, we deplete the heterostructure underneath them, isolating a small droplet of electrons from the remaining 2DEG by tunnel barriers. We make ohmic contacts to the remaining 2DEG regions, which are called the source and drain leads. Using these leads, we are able to apply a voltage bias across the quantum dot and measure the resulting currents. Controlling the voltages on the gates allows us to adjust the tunnel barriers between the dot and the source and drain leads as well as the energy of the electrons in the dot.

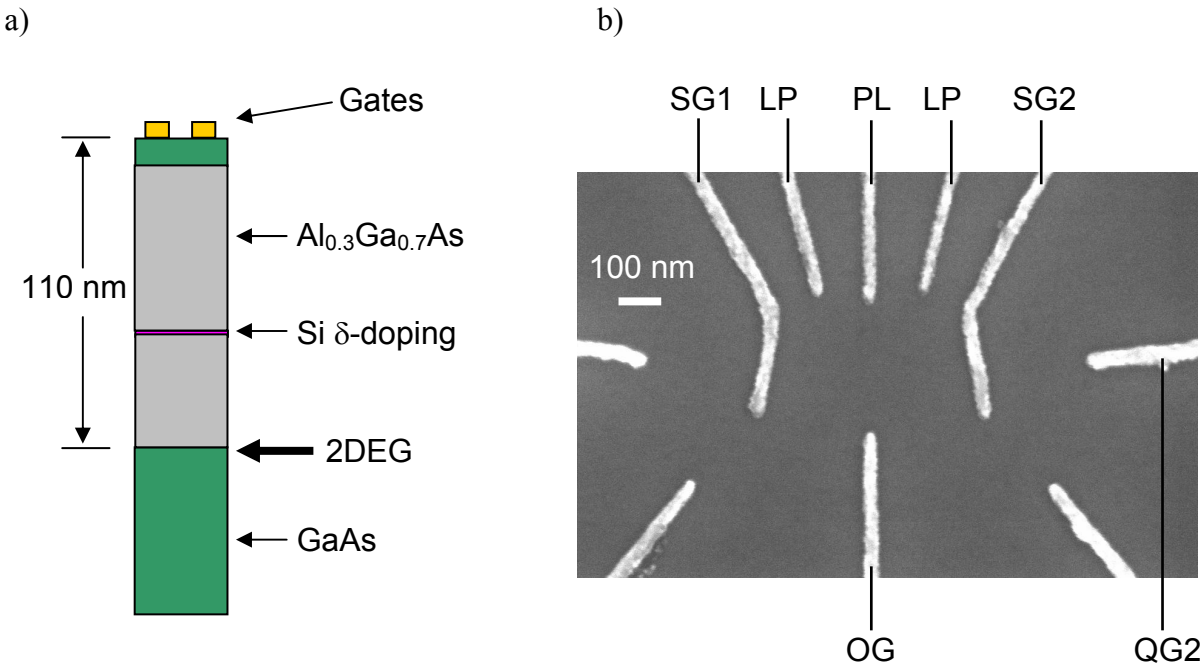

Figure 1: a) Schematic of the heterostructure used in the devices we will study. On top of the heterostructure, we pattern nano-scale metallic gates. b) Electron micrograph of our gate geometry. By applying negative voltages to all the labeled gates except QG2, we are able to form a quantum dot coupled to the remaining 2DEG by tunnel barriers. Applying a negative voltage to QG2 forms a quantum point contact between QG2 and SG2, which is used for charge sensing. Unlabeled gates are not used.

An important feature of SETs is that electrons can be added to the quantum dot one electron at a time[2-4], a phenomenon known as Coulomb blockade. Coulomb blockade occurs because the energy to add an additional electron to the dot is given by $U= e^2/C$, where C is the self-capacitance of the quantum dot. For nano-scale quantum dots like

those used in this work, this energy scale is approximately 2 meV. Since these dots are measured in dilution refrigerators (our electron temperature is 120 mK), this energy scale is much greater than the thermal energy available. Consequently, electrons fill the dot until the energy to add the next electron is above the Fermi energy of the leads, as shown in figure 2a. By applying a more positive gate voltage, we lower the energy of the electrons in the quantum dot relative to the Fermi energy of the leads. When the energy to add the next electron is equal to the Fermi energy in the leads (figure 2b), called the charge degeneracy point, electrons can tunnel onto and off of the dot. Finally, by increasing the gate voltage further, an electron fills the empty level, and the number of electrons on the dot increases by one (figure 2c). It is important to note that electrons can move across the dot only at the charge degeneracy point. Thus we expect the conductance across the quantum dot to be zero, except at charge degeneracy points. This is exactly what we see in the red data in figure 2d, which shows dot conductance as a function of the voltage on one of the gates. The peak marks the voltage at which an additional electron is added to the dot.

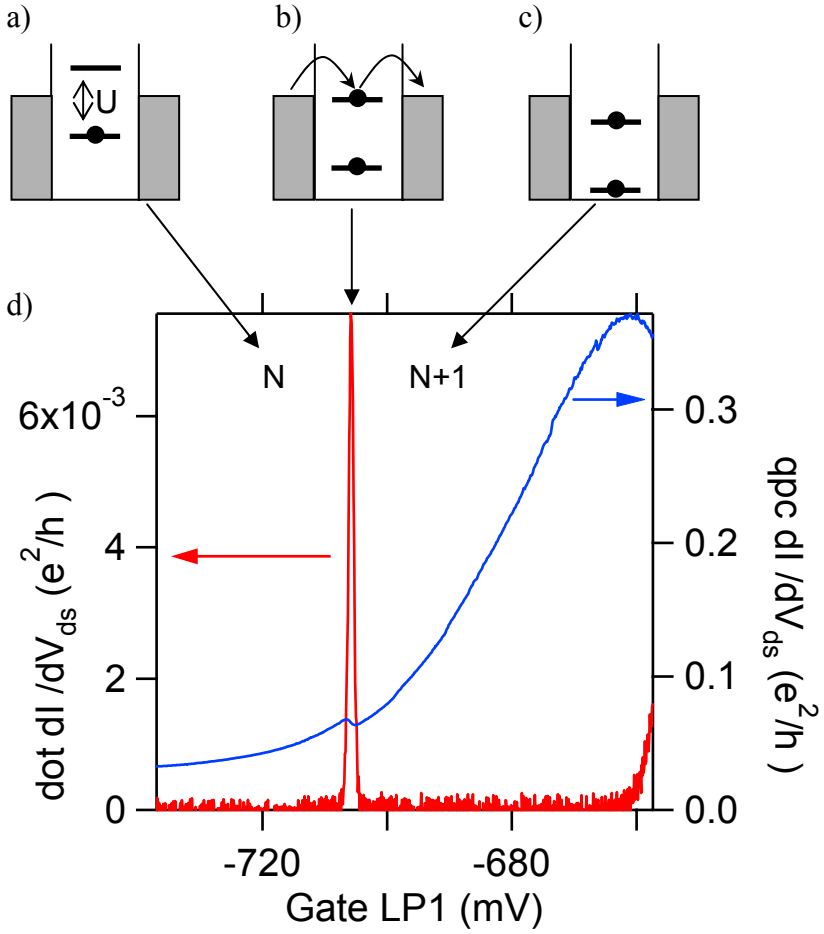

Figure 2: a-c) Dot energy level diagrams. As the gate voltage is made more positive, it reduces the energy of the electrons in the quantum dot and another electron is added to the dot. d) Simultaneous measurement of the conductance of the quantum dot (left scale) and the QPC (right scale). The peak in the dot conductance, which occurs when the dot makes the transition from having N to N+1 electrons, corresponds to a dip in the conductance of the QPC.

Our gate geometry also allows us to form a quantum point contact (QPC) next to the device. Applying a negative voltage to the gate labeled QG2, we create a 1-D channel between SG2 and QG2. The conductance of this channel is decreased by applying a slightly more negative voltage to the either of the gates SG2 or QG2. Similarly, adding an electron to the SET increases the electrochemical potential of the channel and causes the conductance of the QPC to decrease. Thus the QPC serves as a sensitive electrometer for detecting charge on the SET[22]. Figure 2d illustrates this response. The red data show the conductance through the dot, while the blue data show the conductance of the QPC,

which was measured simultaneously. The overall variation in conductance of the QPC is caused by the effect of the gate LP1 on the QPC. However, there is a small dip in the QPC conductance at the position of the peak in the dot conductance data, where the states of the dot with N electrons and N+1 electrons are degenerate. As this additional electron is added, it gates the QPC, reducing the conductance.

To optimize the response of the QPC to the charge on the dot, the dot gates shown in figure 1b are made as thin as possible. This allows the dot and QPC to form closer to one another, increasing the sensitivity of the QPC to the charge on the dot. The geometry of the gates is similar to the geometry first developed by Ciorga, *et al.*[23], which allows one to completely empty the dot. We can then add a single electron to the dot, whose spin we attempt to manipulate with microwave radiation.

3. REAL-TIME READ-OUT

A significant advantage of measuring charge with the QPC is that this method can probe the dot in regimes where conventional transport cannot. Specifically, by applying large enough voltages to SG1, SG2, and OG, we can constrict the tunnel barriers enough to reduce the tunneling rates to the order of 2000 Hz or lower. In this regime, the currents are of order 10^{-16}A, well below the resolution of any available current amplifier. Using the QPC charge sensor, however, we are able to monitor the charge on the dot, even in this weak tunneling regime, and detect fluctuations of charge on the dot. If we make the bandwidth of our detection circuit large enough, we are able to see these charge transitions occur in real time[15].

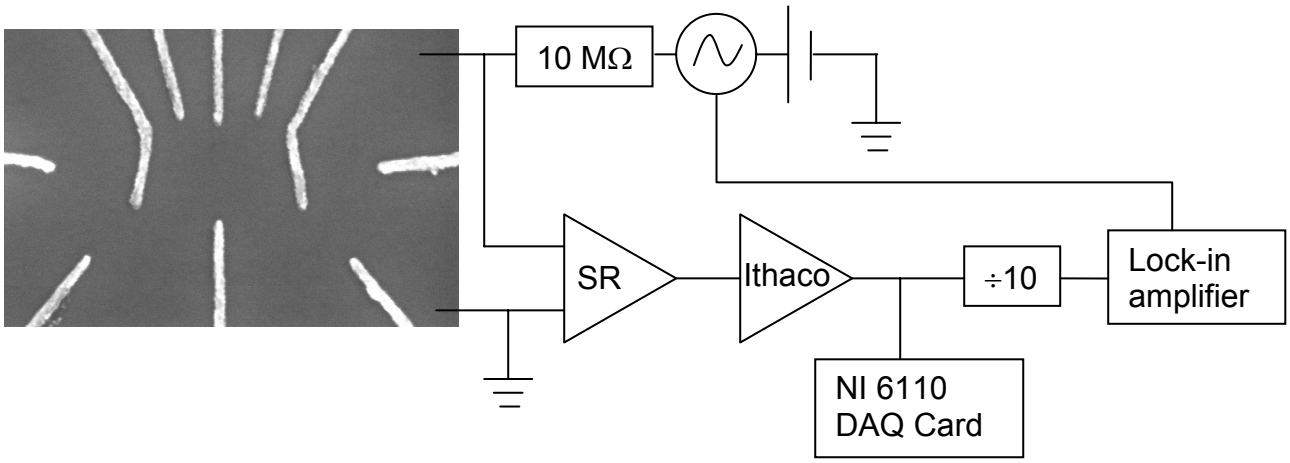

Figure 3: QPC measurement circuit.

The circuit we use for our measurements is sketched in figure 3. We source a dc current of 1 nA for measuring the time-dependent response of the QPC to changes of charge on the dot. We can also add an ac modulation of 0.2 nA to the sourced current for measuring the time averaged resistance of the QPC. The 10MΩ load resistor is mounted on the mixing chamber of the dilution refrigerator, minimizing its Johnson noise. The first stage read-out voltage pre-amplifier, labeled SR on the diagram, is a Signal Recovery Model 5184 which has a fixed gain of 1000. To reduce noise, this amplifier is powered by external batteries. The second stage amplifier, labeled Ithaco in the diagram, is an Ithaco model 1201 voltage pre-amplifier, which is set at a gain of 50. The dc voltage is measured by an NI 6110 DAQ card, which has 12 bit resolution and a range of ±10 V. We typically sample at 500 kHz. In addition to measuring the real-time voltage on the QPC, we can measure the ac component of the signal using an SR830 lock-in amplifier. Since we use a current-biased detection scheme, the bandwidth of our detection is limited by the resistance of the point contact and the capacitance of the signal lines into and out of the dilution refrigerator. We typically operate the QPC at a resistance of 100 kohms, giving a bandwidth of approximately 3 kHz.

Figure 4a shows the charge transition as detected by monitoring the ac voltage across the QPC at 268 Hz and a bandwidth of about 5 Hz. (We convert the measured resistance into a conductance.) With only dc current through the QPC and using the NI DAQ card to monitor the voltage at the output of the second stage amplifier, our bandwidth is greatly increased, and we are able to see charge transitions in real time. These transitions are shown in figure 4b. To determine the rate at which an electron tunnels on and off the dot, we histogram the times spent on and off the dot as shown in figures 4c and 4d. Fitting these data to an exponential allows us to determine the tunneling rates onto and off of the dot.

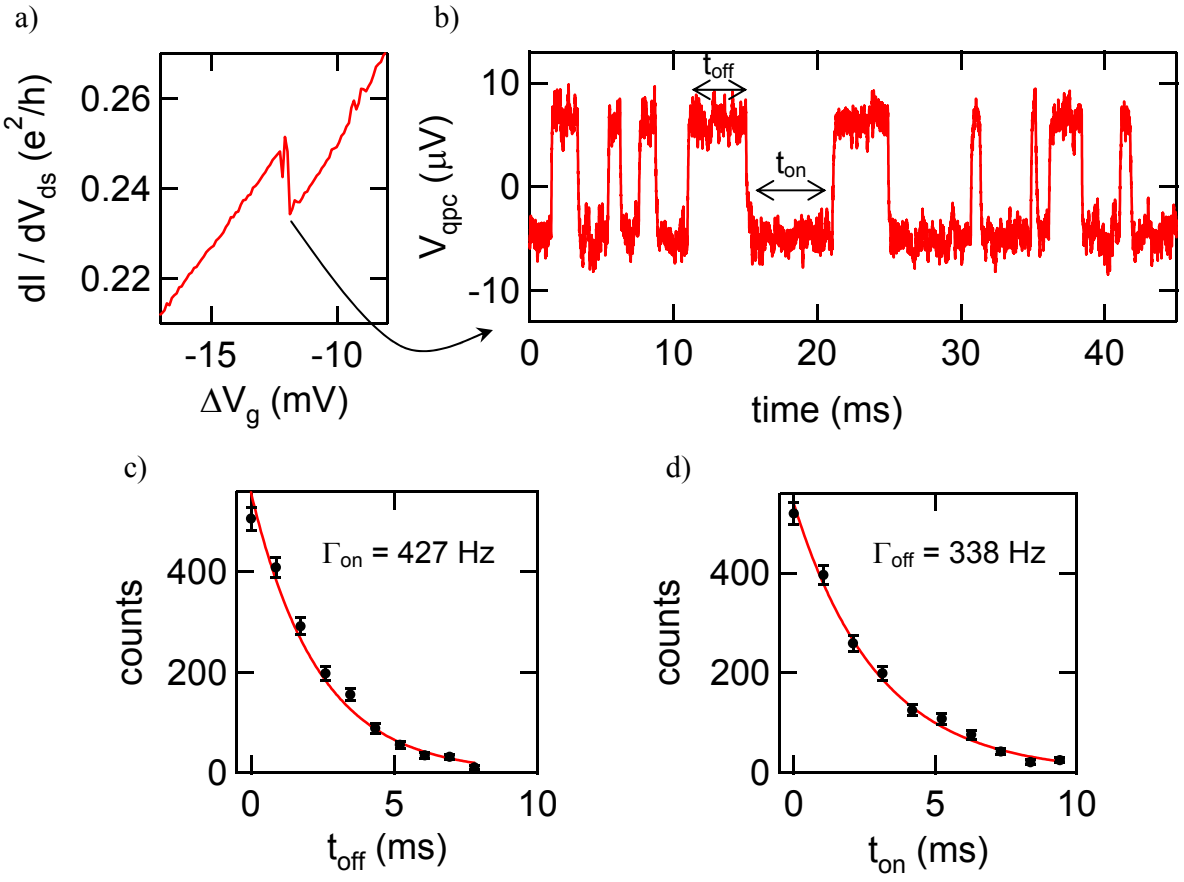

Figure 4: a) Addition of the first electron to the quantum dot as measured by the time-averaged response of QPC charge sensor using limited bandwidth. ΔV_g is the change in gate voltage applied to LP1, PL, and LP2. b) Measurement of the voltage across the QPC with 1 nA applied to it. The charge transitions caused by electrons tunneling on and off the dot are easily visible. The positive voltage state corresponds to an electron being off the dot, while the negative voltage state corresponds to an electron being on the dot. c) and d) Histograms of the off times and on times, respectively, for data like those in b). Fitting the data in c) and d) gives the rates at which electrons tunnel onto and off of the quantum dot, respectively.

4. MICROWAVE EXCITATION

To perform the ESR experiment, we need to expose a quantum dot in a dilution refrigerator to a magnetic field oscillating at microwave frequencies. In order to achieve this goal, we have built and installed a resonant cavity in our dilution refrigerator. Figure 5a illustrates our setup.

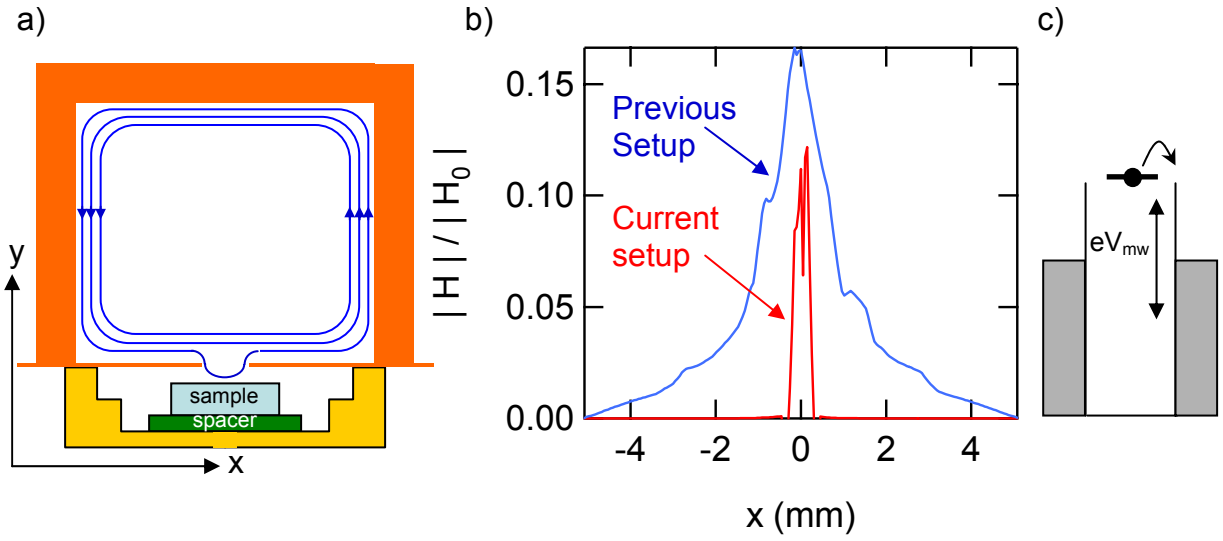

Figure 5: a) Schematic of the setup. The quantum dot sample is positioned 100 μm away from a hole 250 μm in diameter. We excite the TE110 mode of the cavity. The hole is located at a maximum of the magnetic field (and a minimum of the electric field), so the field lines leak out the hole and illuminate the dot. b) Magnetic field at the sample vs distance along the face of the cavity calculated using the HFSS simulation software. $|H_0|$ is the magnetic field that would be at the wall of the cavity if the hole were not present. The hole is centered at 0. The blue curve shows the calculation for the previous setup with a 1500 μm hole used in Kogan *et al.*[14] The red curve shows the calculation for the current setup with the smaller hole. c) Example of how microwave pick-up can lead to ionization of the dot. In this case, the pick-up is shown as being on the gates, although in practice there is pick-up on the source and drain leads as well.

We excite the TE 110 mode of the cavity using a microwave coaxial line going down our dilution refrigerator and coupled to the cavity at the maximum of the electric field. The resonance frequency for this mode is 13.44 GHz and the Q of the cavity is approximately 2000. For the microwave powers we typically use in this experiment, we expect to get $|H_0|$= 6 μT, where $|H_0|$ is defined as the size of the field that would be at the wall of the cavity in the absence of the hole. We mount the quantum dot sample over a 250 μm diameter hole in a thin (25 μm) wall of the cavity where the magnetic field is a maximum and the electric field a minimum. This hole allows the magnetic field lines to leak out of the cavity and illuminate the dot with microwave radiation.

An important design consideration in the assembly of the resonator is the size of the hole. Our previous experiments[14] using a SET approximately 500 μm from a 1500 μm diameter hole suffered from electrical pick-up caused by the magnetic flux lines threading through the wire bonds to the sample. Although the magnetic fields used in these previous experiments were very small, the high frequency plus the large area illuminated by the hole combined to give hundreds of microvolts of pick-up. Pick-up on the source and drain causes an oscillating difference in the Fermi energies of the two leads, while pick-up on the gates causes oscillations in the energy of the electron on the dot relative to both leads. In our previous experiments, the tunneling rate through the barriers was on the order of GHz. Hence the result of the pick-up was that whenever the energy of the electron on the dot exceeded the Fermi energy in one of the leads, the electron tunneled off the dot (see figure 5c). Consequently, the electron did not experience the microwaves long enough to be promoted into the excited state. Also, the currents associated with this ionization process provided a significant background that would have obscured any sign of electron spin resonance.

In order to reduce the magnetic pick-up, we have reduced the size of the hole by a factor of 6, which should lead to a reduction in the area illuminated, and hence the pick-up, by a factor of 36. Since the strength of the magnetic field at a given distance from the hole decreases as the hole is made smaller, we also had to move the dot closer to the hole in order to maintain the strength of the magnetic fields. We have mounted the quantum dot approximately 120 μm from the hole in the resonator wall. Using Ansoft's HFSS simulation package, we have simulated the fields we expect at the

dot given our geometry. The results of this simulation for our current configuration, as well as our previous configuration, are shown in figure 5b.

5. PROPOSED EXPERIMENTS

An example of an ESR measurement sequence is shown below in figure 6. Before we begin, we adjust the voltage on SG1 to reduce the tunnel rate through this barrier to nearly zero. Thus the dot is coupled only to the lead near SG2. The first step is to initialize the dot in the ground state. The static magnetic field splits the spin states of the single electron on the dot by the Zeeman energy, with the excited spin state being $|g|\mu_B B$ above the ground spin state. We adjust the gate voltages to position the energy of the ground spin state below the Fermi energy of the leads, while the excited spin state is just above the Fermi energy of the leads. This configuration suppresses the population of the excited state by the Boltzman factor $\exp(-|g|\mu_B B/k_B T)$. We then apply the microwaves for a period of time t_{mw} = 100 μs. During this time, we typically apply enough power to generate approximately 500 μV of pick-up. In the previous experiment, this level of pick-up created problems as described above. However, in the current experiment the tunnel rates are on the order of kHz rather than GHz. As a result, for a 100 μs microwave exposure time, most electrons cannot tunnel off the dot even if the energy of the electron on the dot exceeds the energy in the leads. During the microwave pulse, the electron on the dot may or may not make a transition to the excited spin state. If it does, then when the microwaves turn off, the energy of the electron will be above the Fermi energy in the lead and we will observe an electron tunneling out of this state. If the electron remains in the ground state, there should be no electron tunneling event.

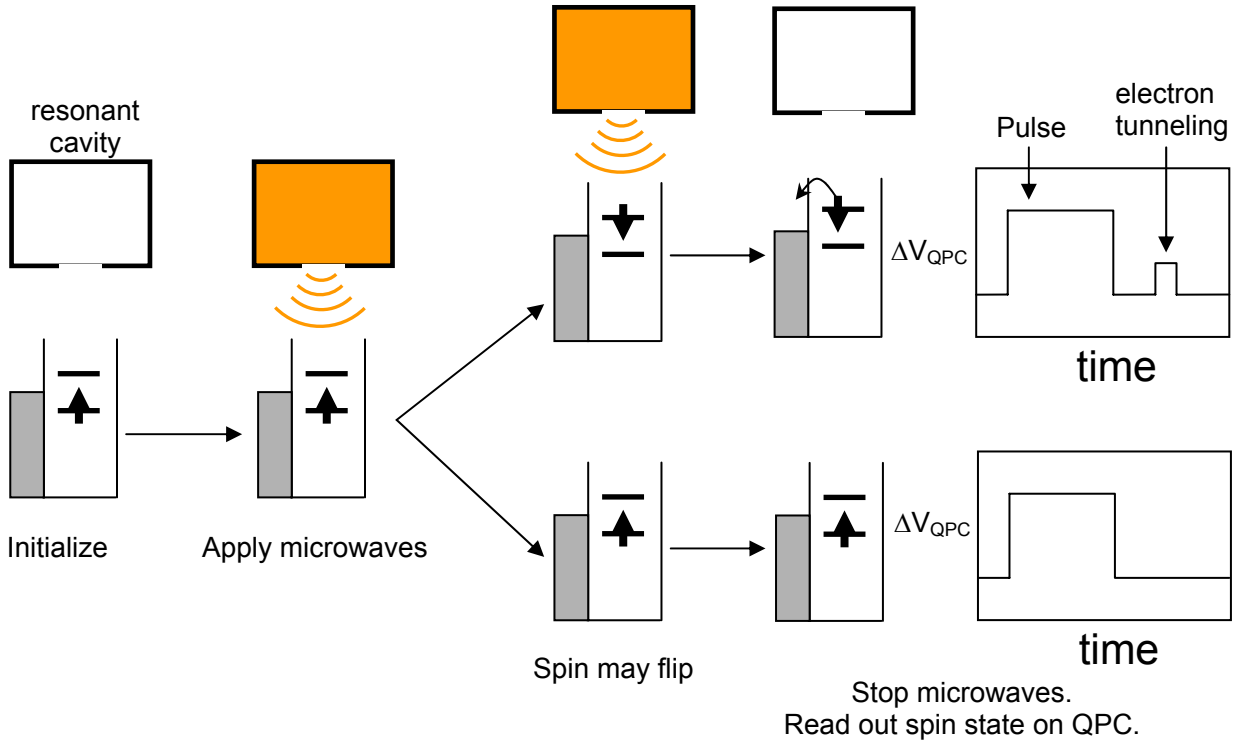

Figure 6: ESR measurement sequence.

Data from such a pulse sequence is shown in figure 7a below. The regularly repeating sharp pulses are the response of the QPC to pick-up during the time the microwaves are applied. The first pulse on the left is an example of an ionization pulse. In this case the electron tunnels off the dot during the microwave pulse, leaving the dot empty. Hence the first tunneling event after the end of the microwave pulse is an electron tunneling onto the empty dot. After the third pulse, we see an electron hopping off the dot, which indicates that the electron in the dot was in the excited state after the microwave pulse; the thermal ionization rate from the ground state is very small.

To search for the resonance between the Zeeman energy and the microwave photon energy as a function of magnetic field, we measure the times between the end of the microwave pulse and when an electron tunnels off the quantum dot at each dc magnetic field. We then look for a magnetic field with an enhanced number of counts immediately after the end of the pulse. We have not yet observed this enhancement. Part of the problem in observing the peak is the number of background counts. To study this, we histogram all the tunnel-off events in a 250 mT range and plot the results in figure 7b. We see an exponential decay on top of an offset. The exponential decay is caused by electrons tunneling out of the excited state, while the offset is caused by thermally activated tunneling out of the ground state.

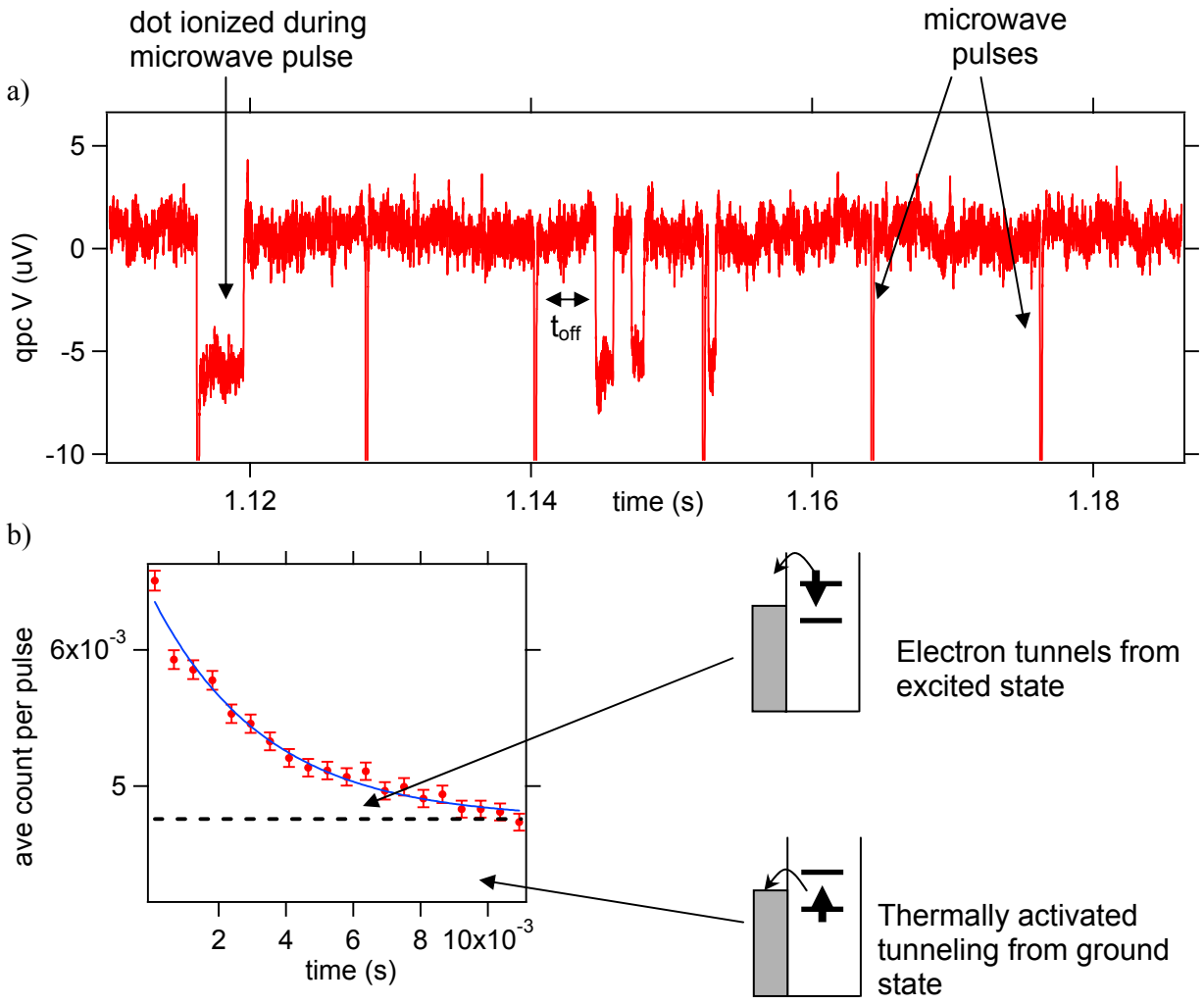

Figure 7: a) Data taken during the ESR measurement sequence. The sharp pulses are the QPC response to the pick-up from the microwaves. The first pulse on the left is an example of an ionization event, where the electron tunnels off the dot during the microwave pulse. After the third microwave pulse, we see that an electron tunnels off the dot a time t_{off} after the pulse ends. This suggests that the electron was in the excited state at the end of the microwave pulse. b) Histogram of all tunnel-off events over a 250 mT range of magnetic field in order to see the relevant backgrounds. The exponential decay is caused by electrons tunneling out of the excited spin state, while the constant offset is from thermally activated tunneling out of the ground state.

The events tunneling out of the excited spin state could have been caused by ESR. However, since the number of these events that we observe is independent of magnetic field over the entire range, these are background events. One possible cause of the excited state background is the ionization events. Although we directly observe some ionization

events, there is also the chance that the dot ionizes and then is re-neutralized by an electron during the microwave pulse, when we cannot observe the charge tunneling off and then back on the dot. An electron filling the dot has an equal probability of tunneling into either the ground or excited state, so this mechanism could leave the dot in the excited state. Another source of the excited state background is the thermal population of the excited state before the microwave pulse is applied.

To help reduce these backgrounds, we can use a modified pulse sequence. Before applying the microwaves, we apply a positive pulse to the gate LP2 to bring the electron in the dot about 1 meV below the Fermi energy of the leads, into the middle of the Coulomb blockade valley. Then we apply the microwaves. Since the level in the dot starts below the energy of the leads, the pick-up caused by the microwaves will not be sufficient to drive the dot levels above the energy of the leads. Finally, we stop applying the microwaves, then the pulse, and bring the dot to the read-out state. We then read out the state of the dot, and look for the ESR signal. This work is currently in progress.

ACKNOWLEDGEMENTS

This work is supported by the Army Research Office (W911NF-05-1-0062), the National Science Foundation (DMR-0353209) and in part by the Nanoscale Science and Engineering Center (NSEC) Program of the National Science Foundation (PHY-0117795).

REFERENCES

1. D. Loss and D. P. DiVincenzo, "Quantum computation with quantum dots", Physical Review A, **57**, 120-126, 1998.
2. M. A. Kastner, "The single-electron transistor", Reviews of Modern Physics, **64**, 849-859, 1992.
3. M. A. Kastner, "Artificial Atoms", Physics Today, 24-31, January 1993.
4. L. P. Kouwenhoven, C. M. Marcus, P. L. McEuen, S. Tarucha, R. M. Westervelt, and N. S. Wingreen, "Electron Transport in Quantum Dots", *Mesoscopic Electron Transport*, L. L. Sohn, L. P. Kouwenhoven, and G. Schön, 105-214, Kluwer Academic Publishers, Dordrecht, 1997.
5. K. Ono, D. G. Austing, Y. Tokura, and S. Tarucha, "Current Rectification by Pauli Exclusion in a Weakly Coupled Double Quantum Dot System", Science, **297**, 1313-1317, 2002.
6. D. M. Zumbühl, J. B. Miller, C. M. Marcus, K. Campman, and A. C. Gossard, "Spin-Orbit Coupling, Antilocalization, and Parallel Magnetic Fields in Quantum Dots", Physical Review Letters, **89**, 276803, 2002.
7. J. Kyriakidis, M. Pioro-Ladriere, M. Ciorga, A. S. Sachrajda, and P. Hawrylak, "Voltage-tunable singlet-triplet transition in lateral quantum dots", Physical Review B, **66**, 035320, 2002.
8. J. A. Folk, R. M. Potok, C. M. Marcus, and V. Umansky, "A Gate-Controlled Bidirectional Spin Filter Using Quantum Coherence", Science, **299**, 679-682, 2003.
9. D. Goldhaber-Gordon, H. Shtrikman, D. Mahalu, D. Abusch-Magder, U. Meirav, and M. A. Kastner, "Kondo effect in a single-electron transistor", Nature, **391**, 156-159, 1998.
10. S. M. Cronenwett, T. H. Oosterkamp, and L. P. Kouwenhoven, "A Tunable Kondo Effect in Quantum Dots", Science, **281**, 540-544, 1998.
11. S. Sasaki, S. De Franceschi, J. M. Elzerman, W. G. van der Wiel, M. Eto, S. Tarucha, and L. P. Kouwenhoven, "Kondo effect in an integer-spin quantum dot", Nature **405**, 764-767, 2000.
12. A. Kogan, G. Granger, M. A. Kastner, D. Goldhaber-Gordon, and H. Shtrikman, "Singlet-triplet transition in a single-electron transistor at zero magnetic field", Physical Review B, **67**, 113309, 2003.
13. D. M. Zumbühl, C. M. Marcus, M. P. Hanson, and A. C. Gossard, "Cotunneling Spectroscopy in Few-Electron Quantum Dots", Physical Review Letters, **93**, 256801, 2004.
14. A. Kogan, S. Amasha, and M. A. Kastner, "Photon-Induced Kondo Satellites in a Single-Electron Transistor", Science, **304**, 1293-1295, 2004.
15. J. M. Elzerman, R. Hanson, L. H. Willems van Beveren, B. Witkamp, L. M. K. Vandersypen, and L. P. Kouwenhoven, "Single-shot read-out of an individual electron spin in a quantum dot", Nature, **430**, 431-435, 2004.
16. V. N. Golovach, A. Khaetskii, and D. Loss, "Phonon-Induced Decay of the Electron Spin in Quantum Dots", Physical Review Letters, **93**, 016601, 2004.
17. S. Amasha, K. MacLean, D. Zumbühl, I. Radu, M. A. Kastner, M. P. Hanson, and A. C. Gossard, in preparation.

18. A. C. Johnson, J. R. Petta, J. M. Taylor, A. Yacoby, M. D. Lukin, C. M. Marcus, M. P. Hanson, and A. C. Gossard, "Triplet-singlet spin relaxation via nuclei in a double quantum dot", Nature, **435**, 925-928, 2005.
19. A. V. Khaetskii, D. Loss, and L. Glazman, "Electron Spin Decoherence in Quantum Dots due to Interaction with Nuclei", Physical Review Letters, **88**, 186802, 2002.
20. J. R. Petta, A. C. Johnson, J. M. Taylor, E. A. Laird, A. Yacoby, M. D. Lukin, C. M. Marcus, M. P. Hanson, and A. C. Gossard, "Coherent Manipulation of Coupled Electron Spins in Semiconductor Quantum Dots", Science, **309**, 2180-2184.
21. H.-A. Engel and D. Loss, "Detection of Single Spin Decoherence in a Quantum Dot via Charge Currents", Physical Review Letters, **86**, 4648-4651, 2001.
22. M. Field, C. G. Smith, M. Pepper, D. A. Ritchie, J. E. F. Frost, G. A. C. Jones, and D. G. Hasko, "Measurements of Coulomb Blockade with a Noninvasive Voltage Probe", Physical Review Letters, **70**, 1311-1314, 1993.
23. M. Ciorga, A. S. Sachrajda, P. Hawrylak, C. Gould, P. Zawadzki, S. Jullian, Y. Feng, and Z. Wasilewski, "Addition spectrum of a lateral dot from Coulomb and spin-blockade spectroscopy", Physcial Review B, **61**, R16315-R16318, 2000.

*samasha@mit.edu